

Monte Carlo studies of a Laplacian roughening model for two-dimensional melting

Katherine J. Strandburg, Sara A. Solla, and G. V. Chester
Laboratory of Atomic and Solid State Physics and Materials Science Center,
Cornell University, Ithaca, New York 14853
 (Received 23 May 1983)

Monte Carlo simulations are used to study the thermodynamic properties of the Laplacian roughening model. Nelson has shown that this model is related via a duality transformation to a gas of disclinations in a two-dimensional solid, and mimics the positional and orientational symmetries relevant to two-dimensional melting. In our simulations thermodynamic functions vary continuously over the full temperature range and agree with analytic results at low and high temperatures. Correlation functions exhibit three distinct regimes as a function of temperature and yield strong evidence for the existence of an intermediate phase characterized by short-range positional order and quasi-long-range orientational order. The Monte Carlo results are in quantitative agreement with the predictions of the Kosterlitz-Thouless-Halperin-Nelson-Young theory and establish the existence of two successive continuous phase transitions for the Laplacian roughening model. The corresponding transition temperatures are obtained from the temperature dependence of the renormalized elastic constant K_R and the Frank constant K_A .

I. INTRODUCTION

The nature of the two-dimensional (2D) melting transition has been a matter of considerable controversy since the development of the dislocation-mediated melting theory by Kosterlitz, Thouless, Halperin, Nelson, and Young (KTHNY).¹⁻⁴ Computer simulations and experiments have not always led to unambiguous answers.⁵ Many of the simulations have led to inconclusive results due to finite-size effects and fluctuations on time scales comparable to practical simulation times. Although some computer studies are consistent with the KTHNY theory, most simulations indicate a first-order melting transition.⁶ Several experiments seem to favor dislocation-mediated melting.⁵ The experiments have been performed either on systems such as liquid crystals in which the molecules themselves have inherent angular degrees of freedom,⁷ or on systems such as noble gases adsorbed on graphite in which some external angular order is imposed by the substrate.⁸ A recent experiment⁹ supports the description of 2D melting as a two-step process with an intermediate hexatic phase separating solid from liquid. The data suggest that the hexatic phase exists as a consequence of melting, not as a consequence of the substrate interaction.

Recently Nelson has proposed the Laplacian roughening model,¹⁰ a modification of the solid-on-solid model for interfacial roughening, which is related by a duality transformation to the disclination Hamiltonian of the melting problem. A similar relationship exists between the 2D XY spin model and the gradient roughening model.¹¹ Simulations performed in the gradient roughening model have advanced the understanding of the 2D XY model.¹² We have performed simulations of the Laplacian roughening model to investigate the thermodynamic properties of the disclination system and the mechanism for melting in two dimensions.

A theoretical description of the melting of a 2D elastic solid requires a mechanism for the destruction of the quasi-long-range translational order and the long-range bond angular order characteristic of the solid phase.¹³ (Quasi-long-range order refers to the algebraic decay of the appropriate correlation function.) Kosterlitz and Thouless¹ (KT) proposed a dislocation unbinding mechanism which leads to a continuous transition into a phase characterized by short-range translational order. Halperin and Nelson^{2,3} and Young⁴ (HNY) found that quasi-long-range bond angular order persists in the presence of free dislocations. Each dislocation is a tightly bound disclination pair, and a second continuous transition associated with the unbinding of disclinations takes the system into an isotropic fluid phase. The KTHNY theory for two-dimensional melting thus predicts two successive continuous transitions and an intermediate hexatic phase characterized by short-range translational order and quasi-long-range bond angular order. An alternative mechanism for melting via the nucleation of grain boundaries¹⁴ predicts a single first-order transition from a 2D solid into an isotropic fluid. Grain boundaries are a collective excitation of the disclination system that might preempt the KT transition if the core energy of disclinations is small enough.¹⁵ A better understanding of the thermodynamic properties of the disclination system should enhance the understanding of the problem of melting in two dimensions.

The Hamiltonian for the Laplacian roughening model is¹⁰

$$H_{LR} = (J/2k_B T) \sum_{\vec{r}} |\Delta h(\vec{r})|^2, \quad (1.1)$$

where

$$\Delta h(\vec{r}) = \frac{2}{3} \left[\sum_j [h(\vec{r} + \hat{\delta}_j) - h(\vec{r})] \right]. \quad (1.2)$$

The $\{\hat{\delta}_j\}$ are the six nearest-neighbor vectors in a triangular lattice (see Fig. 1) and the integer $h(\vec{r})$ is the height of the interface at site \vec{r} . The quadratic Hamiltonian (1.1) may be diagonalized by a Fourier transform to give

$$H_{\text{LR}} = (J/2k_B T) \sum_{\vec{q}} G^{-2}(\vec{q}) |h(\vec{q})|^2, \quad (1.3)$$

where

$$h(\vec{q}) = (1/N^{1/2}) \sum_{\vec{r}} h(\vec{r}) \exp(i\vec{q} \cdot \vec{r})$$

and

$$G(\vec{q}) = \left\{ 4 - \frac{4}{3} [\cos(\hat{\delta}_1 \cdot \vec{q}) + \cos(\hat{\delta}_2 \cdot \vec{q}) + \cos(\hat{\delta}_3 \cdot \vec{q})] \right\}^{-1} \quad (1.4)$$

is the triangular lattice Green's function.

A duality transformation applied to the partition function of the Laplacian roughening model leads to an exact factorization into high-temperature and disclination contributions, $Z = Z_{\text{HT}} Z_D$.¹⁰ The high-temperature approximation Z_{HT} is obtained by treating the $\{h(\vec{r})\}$ as continuous variables and performing the resulting Gaussian integrals. The remaining contribution Z_D to the partition function is described by the Hamiltonian

$$H = (2\pi^2 k_B T/J) \sum_{\vec{r} \neq \vec{r}'} V(\vec{r} - \vec{r}') s(\vec{r}) s(\vec{r}'), \quad (1.5)$$

where

$$V(\vec{r}) = (1/N) \sum_{\vec{q}} G^2(\vec{q}) [\exp(i\vec{q} \cdot \vec{r}) + \frac{1}{2}(\vec{q} \cdot \vec{r})^2 - 1] \quad (1.6)$$

and the $\{s(\vec{r})\}$ are integers satisfying the restrictions

$$\sum_{\vec{r}} s(\vec{r}) = 0 \quad (\text{charge neutrality}), \quad (1.7a)$$

$$\sum_{\vec{r}} \vec{r} s(\vec{r}) = 0 \quad (\text{dipole neutrality}). \quad (1.7b)$$

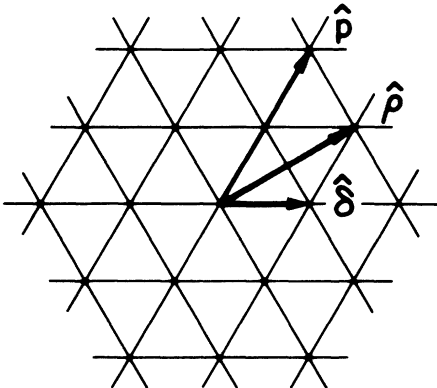


FIG. 1. Nearest-neighbor $\hat{\delta}$, next-nearest-neighbor $\hat{\rho}$, and second-nearest-neighbor $\hat{\rho}$ vectors for the triangular lattice.

For large r , $V(\vec{r})$ has the form

$$V(r) = (3^{1/2}/16\pi)(r^2 \ln r + Ar^2 - B), \quad (1.8)$$

where A and B are lattice-dependent positive constants. This interaction has exactly the same form as the disclination Hamiltonian¹⁰

$$H_D = (\tilde{K}/16\pi k_B \tilde{T}) \sum_{\vec{r} \neq \vec{r}'} |\vec{r} - \vec{r}'|^2 \ln |\vec{r} - \vec{r}'| s(\vec{r}) s(\vec{r}') + (E_c/k_B \tilde{T}) \sum_{\vec{r}} s^2(\vec{r}), \quad (1.9)$$

with elastic constant

$$K = \tilde{K}/k_B \tilde{T} = 2(3^{1/2})\pi^2 k_B T/J,$$

and core energy $E_c = B\tilde{K}/16\pi$, and where $s(\vec{r})$ is the disclination charge at site \vec{r} . Note that the duality transformation maps high temperatures T in the Laplacian roughening model onto low temperatures \tilde{T} in the disclination model and vice versa. Note also that the r^2 term in (1.8) makes no contribution to the partition function when charge and dipole neutrality are imposed. The core energy E_c depends on the lattice geometry and is fixed by the transformation. Thus study of the Laplacian roughening model provides information about the behavior of the disclination system at a fixed core energy.

The Laplacian roughening model may display one or two transitions and can display behavior analogous to grain boundary melting or KTHNY melting. In the KTHNY description, the first of the two transitions corresponds to the system becoming rough and to the orientational ("tilt") order becoming quasi-long-range rather than long range as in the low-temperature phase. The second transition corresponds to the loss of the orientational ("tilt") quasi-long-range order. The smooth, oriented low-temperature phase corresponds by duality to the isotropic fluid phase in the melting problem and the rough, unoriented high-temperature phase corresponds to the solid. The rough but quasioriented phase corresponds to the hexatic phase. The correspondence between the transitions of the disclination system and those of the Laplacian roughening model¹⁰ is summarized in Fig. 2.

The possibility of two transitions is due to a competition between nearest-neighbor and more-distant-neighbor terms in the Hamiltonian, as can be seen by rearranging the Hamiltonian to obtain

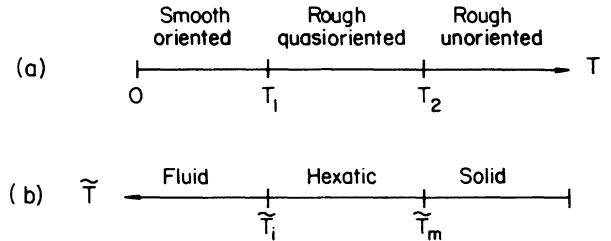


FIG. 2. Correspondence between (a) the phase diagram of the Laplacian roughening model as a function of temperature T , and (b) that of the dual disclination system as a function of temperature \tilde{T} , as predicted by the KTHNY theory of melting.

$$H = (2J/9k_B T) \sum_{\vec{r}} \left[5 \sum_j [h(\vec{r}) - h(\vec{r} + \hat{\delta}_j)]^2 - \sum_j [h(\vec{r}) - h(\vec{r} + \hat{\rho}_j)]^2 - \frac{1}{2} \sum_j [h(\vec{r}) - h(\vec{r} + \hat{p}_j)]^2 \right], \quad (1.10)$$

where the $\{\hat{\delta}_j\}$, $\{\hat{\rho}_j\}$, and $\{\hat{p}_j\}$ are the nearest-, next-nearest-, and second-nearest-neighbor vectors in a triangular lattice, respectively (see Fig. 1). The gradient roughening model (which exhibits only one continuous transition¹²) is recovered if the second and third terms in (1.10) are neglected.

In this paper we report the results of a Monte Carlo simulation of the Laplacian roughening model on a triangular lattice. We have found this model to be very well behaved in simulations. The high- and low-temperature behavior may be calculated analytically including an exact treatment of finite-size effects. Our results confirm the existence of two continuous transitions. We find a roughening transition at $T_1^* = 1.84 \pm 0.01$ and an orientational transition at $T_2^* = 1.925 \pm 0.015$, where T^* is the dimensionless temperature unit $k_B T/J$. The behavior in each of the three phases is in good agreement with the predictions of the KTHNY theory.

Our simulations were performed on a 32×32 ($N = 1024$) triangular lattice with periodic boundary conditions. The Monte Carlo runs usually included an average over 20 000–50 000 passes through the system for thermodynamic quantities and correlation functions. At temperatures near the transitions the configurations were equilibrated for a total of 50 000–100 000 passes. Except where otherwise indicated, the error bars were estimated by averaging groups of 2000 passes and computing the standard deviation treating these “block” averages as independent measurements.

In Sec. II we present our results for local thermodynamic quantities: (i) the internal energy E , (ii) the interface width

$$w = \langle [h(\vec{r}) - \bar{h}]^2 \rangle, \quad (1.11)$$

where \bar{h} is the average height of a particular configuration and $\langle \dots \rangle$ denotes an ensemble average, and (iii) a measure τ of local fluctuations in tilt defined by

$$\tau = \left\langle \left[\sum_j (-1)^j h(\vec{r} + \hat{\delta}_j) \right]^2 \right\rangle. \quad (1.12)$$

In Sec. III we present our results for the following:

(i) The height-height correlation function

$$H(\vec{r}) = \langle [h(\vec{r}) - h(\vec{0})]^2 \rangle. \quad (1.13)$$

This correlation function will remain finite at large r below a roughening transition and will diverge as r tends to infinity in a rough phase. In this model $H(\vec{r})$ is related by duality to the free energy of a pair of oppositely

charged disclinations separated by a distance r [Fig. 3(a)]. The KTHNY picture predicts that this energy diverges at large r throughout the solid (rough, unoriented) and hexatic (rough, quasioriented) phases but remains finite in the fluid (smooth, oriented) phase,¹³ thus establishing the correspondence between the roughening transition and the disclination unbinding transition.

(ii) The tilt-tilt correlation function

$$g(\vec{r}) = \sum_j \langle [h(\vec{r}) - h(\vec{r} + \hat{\delta}_j) - h(\vec{0}) + h(\hat{\delta}_j)]^2 \rangle. \quad (1.14)$$

This correlation function will remain finite at large r in an oriented phase, and will diverge as r tends to infinity in an unoriented phase. In this model $g(\vec{r})$ is related by duality to the free energy of two dislocations (each of them a tightly bound disclination pair) separated by a distance r [Fig. 3(b)].¹⁰ The KTHNY picture predicts that this energy diverges at large r in the solid (rough, unoriented) phase and remains finite in the hexatic (rough, quasioriented) and fluid (smooth, oriented) phases.¹³ The loss of orientational quasi-long-range order in the roughening model thus corresponds to the dislocation unbinding transition.

(iii) The correlation functions

$$c_k(r) = \left\langle \exp \left[2\pi i k \sum_j (-1)^j h(\vec{r}_j) \right] \right\rangle \quad (1.15)$$

and

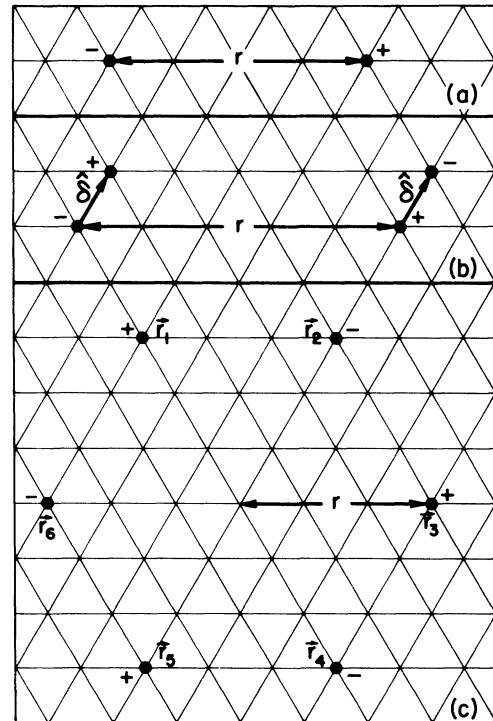


FIG. 3. Configurations of disclination charges corresponding to (a) the height-height correlation function $H(r)$, (b) the tilt-tilt correlation function $g(r)$, and (c) the orientational correlation functions $c_k(r)$ and $c(r)$.

$$c(r) = \left\langle \left[\sum_j (-1)^j h(\vec{r}_j) \right]^2 \right\rangle \quad (1.16)$$

(corresponding to τ), where the \vec{r}_j are situated on a hexagon of linear size r [Fig. 3(c)]. These correlation functions are related by duality to the free energy of six disclinations arranged in a hexagon of size r [Fig. 3(c)].¹⁰ This configuration of disclinations can be viewed as three dislocations. As r increases, both the dislocations, and the disclinations within a given dislocation, are pulled apart. Thus these correlation functions are sensitive to both the disclination unbinding and dislocation unbinding transitions.

In Sec. IV we make a quantitative comparison of our correlation-function results with the predictions of the KTHNY theory.¹³ Within the KTHNY picture, we calculate finite-size forms for these functions in all three phases.^{15,16} Our Monte Carlo results give good fits to the predicted forms. Using these forms, we extract renormalized values for the elastic constant K and the Frank constant K_A as a function of temperature. HNY predict that $K_R \rightarrow 16\pi$ at T_2^* (corresponding to the dislocation unbinding transition at \tilde{T}_m) and that $K_A \rightarrow 72/\pi$ at T_1^* (corresponding to the disclination unbinding transition at \tilde{T}_i).^{2,3} We find good agreement with these predictions.

II. LOCAL THERMODYNAMIC QUANTITIES

A. Internal energy

We have computed the energy per site of the Laplacian roughening model by Monte Carlo simulation and by low- and high-temperature approximations. The low-temperature expansion obtained by considering the lowest-energy excitations yields the expression

$$\begin{aligned} E/J = & \left(\frac{2}{3}\right)^2 [42X^{21} + 192X^{32} + 132X^{33} + 216X^{36} + 720X^{40} \\ & + 246X^{41} - 1512X^{42} + 258X^{43} + 1056X^{44} \\ & + 720X^{45} + 552X^{46} + 1692X^{47} \\ & + 576X^{48} + o(X^{50})], \end{aligned} \quad (2.1)$$

where $X = \exp(-\frac{4}{9}T^{*-1})$, and $T^* = k_B T/J$.

The high-temperature approximation described in Sec. I yields

$$E = \frac{1}{2}k_B T \text{ and } E^* = E/J = \frac{1}{2}T^*. \quad (2.2)$$

Our Monte Carlo results are shown in Fig. 4. We find excellent agreement with the low-temperature expansion for $T^* < 1.65$ and with the high-temperature result for $T^* > 2.25$, with a rapid continuous rise in between.

We have calculated the specific heat by computing $\Delta E^*/\Delta T^*$. The result is shown in Fig. 5. We see one rather narrow peak at T^* approximately equal to 1.85. There may possibly be a shoulder on the high-temperature side of the peak near $T^* = 1.9$, but the resolution of our computations does not allow us to make a conclusive statement about this possibility.

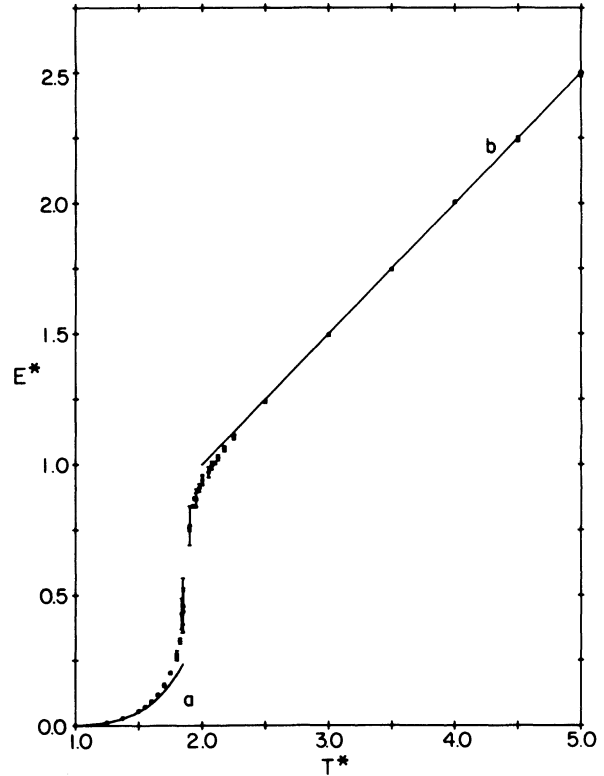


FIG. 4. Internal energy E^* as a function of temperature T^* . The Monte Carlo data are shown and compared with the low-temperature expansion (curve *a*) and the high-temperature approximation (curve *b*).

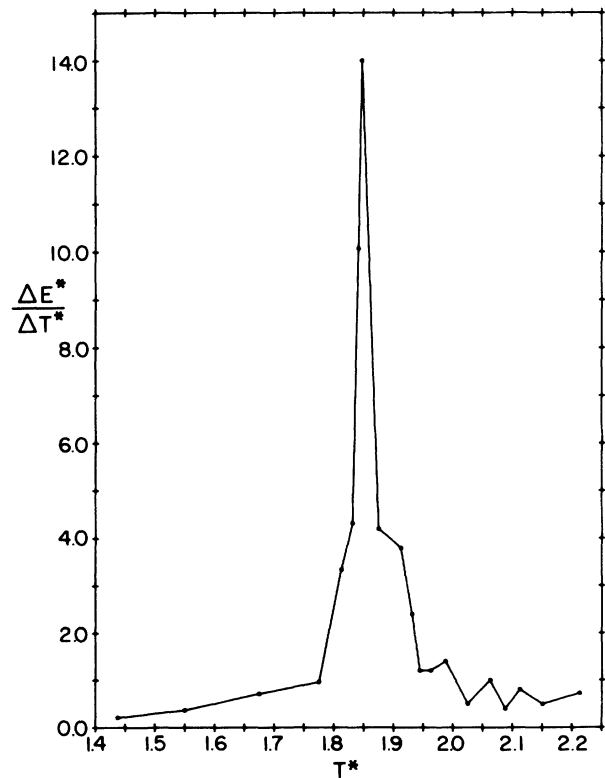


FIG. 5. Specific heat $\Delta E^*/\Delta T^*$ as a function of temperature T^* . The solid curve is composed of straight lines between neighboring data points.

B. Interface width

As a measure of surface roughness we have computed the interface width defined by

$$w = (1/N) \left\langle \sum_{\vec{r}} [h(\vec{r}) - \bar{h}]^2 \right\rangle, \quad (2.3)$$

where \bar{h} is the average height of a particular configuration. We have subtracted the average height for each configuration to cancel the effect of possible long-time fluctuations of \bar{h} away from zero.¹⁷ Our Monte Carlo results are shown in Fig. 6.

The low-temperature expansion for this quantity is

$$\begin{aligned} w = & 2X^{21} + 12X^{32} + 12X^{33} + 24X^{36} + 72X^{40} + 12X^{41} \\ & - 62X^{42} + 12X^{43} + 102X^{44} + 60X^{45} + 72X^{46} \\ & + 192X^{47} + 84X^{48} + o(X^{50}). \end{aligned} \quad (2.4)$$

Our Monte Carlo results are in excellent agreement with this expansion for $T^* < 1.65$.

The high-temperature approximation described in Sec. I yields

$$w = (T^*/N) \sum_{\vec{q}} G^2(\vec{q}), \quad (2.5)$$

where $G(\vec{q})$ is given by (1.4). Above the roughening tem-

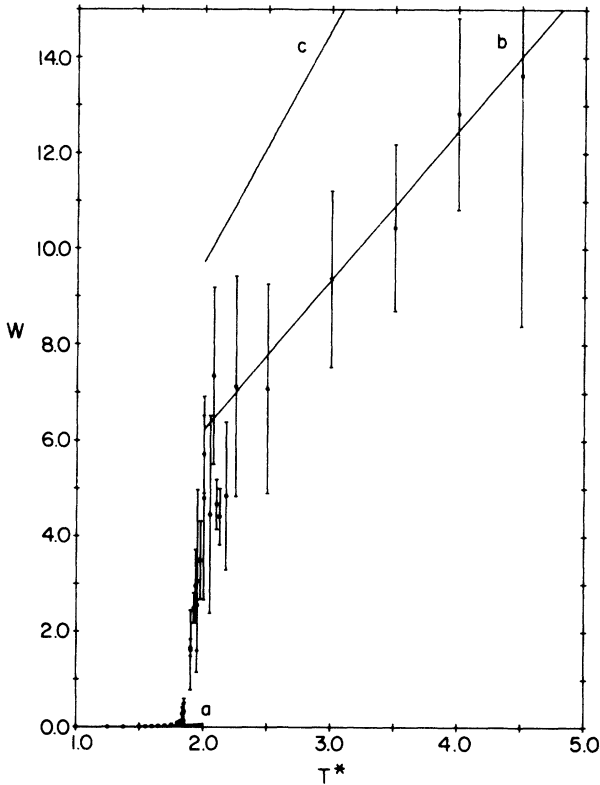


FIG. 6. Interface width w as a function of temperature T^* . The Monte Carlo data are shown and compared with the low-temperature expansion (curve *a*), the high-temperature approximation (2.5) for a finite system with periodic boundary conditions (curve *b*), and the integral approximation (2.6) to the high-temperature result (curve *c*).

perature the interface width diverges linearly with N . This divergence is due to the fact that $G(\vec{q})$ diverges as $1/q^2$ for small q . In a finite system, however, the width is bounded even when the interface is rough. The sum in (2.5) may be evaluated by an integral approximation assuming the small- q form for $G(\vec{q})$ (since small q is the major contribution to the integral) and a circular Brillouin zone of radius $(8\pi/3^{1/2})^{1/2}$ chosen to preserve the zone area. This integral approximation yields

$$w = T^*(6N/128\pi^2) = 4.86T^* \quad \text{for } N = 1024. \quad (2.6)$$

As is clear from Fig. 6 this integral approximation does not give good agreement with our Monte Carlo results.

We therefore evaluate the sum over \vec{q} in (2.5) exactly for a finite-size system with periodic boundary conditions to obtain

$$w = 3.114T^* \quad \text{for } N = 1024. \quad (2.7)$$

This form is in good agreement with our Monte Carlo data for $T^* > 2.25$. The average values are within 5% of the predictions given by (2.7). The fluctuations in these values are quite large and increase with temperature. These large fluctuations are due to the fact that the width is sensitive to long-wavelength modes. Fluctuations in the interface width are given in the high-temperature approximation by $\Delta w = (2^{1/2})w$. In this temperature regime both w and Δw are predicted to grow linearly with temperature for a finite-size system.

C. Local orientation

A local measure of the fluctuations in the surface orientation is given by

$$\tau = (1/N) \left\langle \sum_{\vec{r}} \left[\sum_j (-1)^j h(\vec{r} + \hat{\delta}_j) \right]^2 \right\rangle, \quad (2.8)$$

where the $\{\hat{\delta}_j\}$ are the six nearest-neighbor vectors. Note that τ is not sensitive to a uniform tilt of the nearest-neighbor hexagon, and is therefore a measure of a very different character than w .

The low-temperature expansion for this quantity is

$$\begin{aligned} \tau = & 12X^{21} + 48X^{32} + 24X^{33} + 48X^{36} + 144X^{40} + 84X^{41} \\ & - 432X^{42} + 60X^{43} + 240X^{44} + 192X^{45} + 144X^{46} \\ & + 360X^{47} + 96X^{48} + o(X^{50}). \end{aligned} \quad (2.9)$$

The high-temperature approximation is

$$\begin{aligned} \tau = (T^*/N) \sum_{\vec{q}} G^2(\vec{q}) \left[6 - 2 \sum_j e^{i\vec{q} \cdot \hat{\delta}_j} \right. \\ \left. + 2 \sum_j e^{i\vec{q} \cdot \hat{\rho}_j} - \sum_j e^{i\vec{q} \cdot \hat{p}_j} \right], \end{aligned} \quad (2.10)$$

where $\{\hat{\delta}_j\}$, $\{\hat{\rho}_j\}$, and $\{\hat{p}_j\}$ correspond to the six nearest-, next-nearest-, and second-nearest-neighbor vectors, respectively (see Fig. 1). Approximating the sum by an integral, as described above, yields

$$\tau = [\pi/8(3^{1/2})]T^* = 0.226T^*, \quad (2.11)$$

independent of N , whereas summing numerically yields

$$\tau = 0.230T^* \quad (2.12)$$

for $N = 1024$. The results (2.11) and (2.12) agree quite well with one another since τ is a truly local quantity and is not sensitive to long-wavelength modes.

Figure 7 shows our results for τ . The agreement with high- and low-temperature results is excellent for $T^* > 2.25$ and for $T^* < 1.65$, respectively, as already observed for the internal energy and interface width.

Our determination of local thermodynamic quantities demonstrates that the Laplacian roughening model is well suited to Monte Carlo simulation. We conclude from these quantities that if there are two transitions they occur between $T^* = 1.65$ and $T^* = 2.25$. All three of the local quantities computed show very similar temperature dependence. All three quantities have been determined both by heating from a perfectly flat interface and by cooling from an equilibrated configuration at high temperature. We see no hysteresis in any of these quantities.

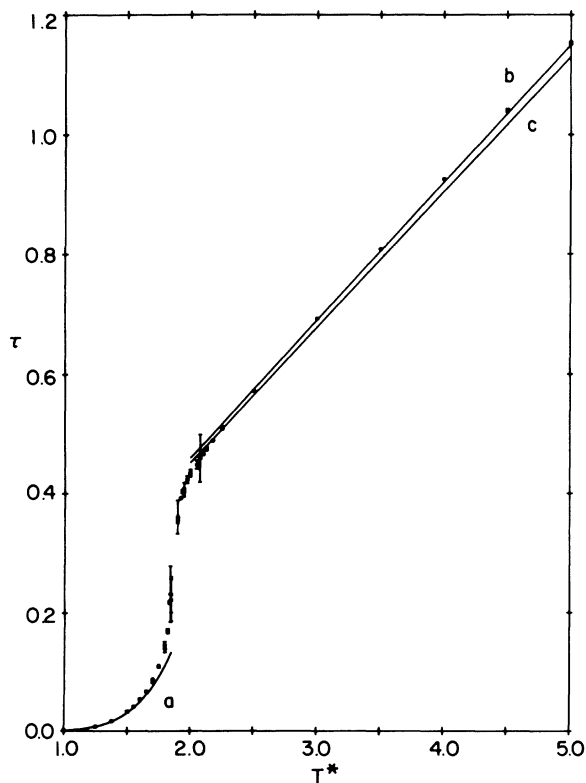


FIG. 7. Local tilt fluctuations τ as a function of temperature T^* . The Monte Carlo data are shown and compared with the low-temperature expansion (curve *a*), the high-temperature approximation (2.10) for a finite system with periodic boundary conditions (curve *b*), and the integral approximation (2.11) to the high-temperature result (curve *c*).

III. CORRELATION FUNCTIONS

A. Height-height correlation function

The height-height correlation function, defined as

$$H(\vec{r}) = \langle [h(\vec{r}) - h(\vec{0})]^2 \rangle, \quad (3.1)$$

is sensitive to the roughening transition. The high-temperature approximation is

$$H(\vec{r}) = (2T^*/N) \sum_{\vec{q}} G^2(\vec{q}) [1 - \exp(i\vec{q} \cdot \vec{r})]. \quad (3.2)$$

The integral approximation to (3.2) yields

$$H(r)/T^* = (3^{1/2}/8\pi) [r^2 \ln(N^{1/2}/r) - Ar^2 + B], \quad (3.3)$$

where A and B are the same constants which appear in the interaction $V(r)$ given in (1.8). Note that in the thermodynamic limit $H(r)$ diverges as $\ln N$ for all r at high temperatures.

Figure 8 shows our Monte Carlo results for the height-height correlation function. At low temperatures the height-height correlation function should approach a finite asymptotic value. The curves for $T^* < 1.8$ clearly show this behavior. In addition, we have plotted the exact finite-size high-temperature form (3.2) for a 32×32 system. Despite rather large fluctuations at large r it is clear that the high-temperature result fits the data well for

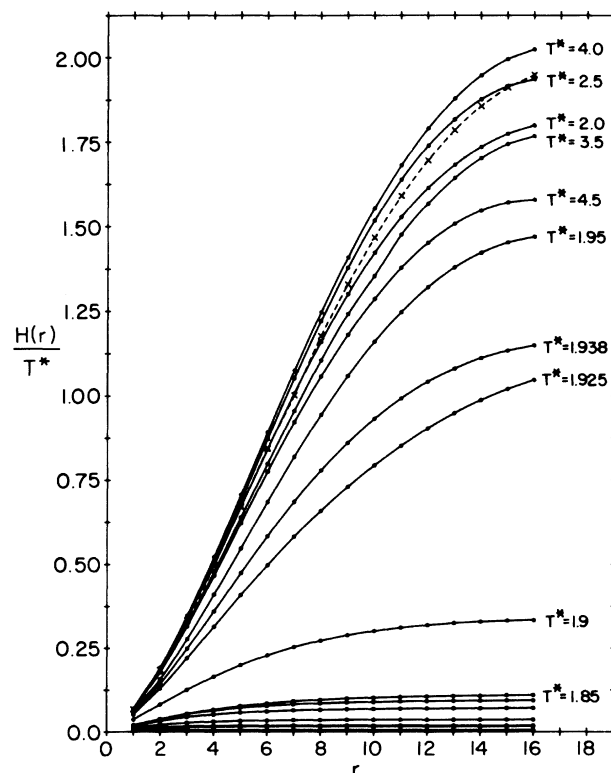


FIG. 8. Monte Carlo data for the height-height correlation function $H(r)$ as a function of separation r at various temperatures T^* . The curve $\times \cdots \times$ represents the high-temperature approximation (3.2) for a finite system with periodic boundary conditions.

TABLE I. Monte Carlo results for w and $H(r=16)$ for low and high temperatures, and the values for $\langle h(\vec{r})h(\vec{0}) \rangle$ at $r=16$ which follow from Eq. (3.4).

T^*	w	$H(16)$	$\frac{1}{2}[2w - H(16)]$	$\langle h(0)h(16) \rangle$ (high T^*)
1.6	0.016	0.032	0.000	
1.75	0.056	0.114	-0.001	
1.8	0.065	0.132	-0.001	
1.825	0.138	0.264	0.006	
2.0	6.10	15.48	-1.64	-1.56
2.5	7.08	18.00	-1.92	-1.96
3.5	10.36	22.08	-0.68	-2.74
4.0	12.90	32.38	-3.29	-3.12
4.5	13.50	31.80	-2.40	-3.52

$T^* > 2.0$. In addition, the data at $T^* = 1.95$ and $T^* = 1.938$ show the same shape as that in the high-temperature region.

As an additional check on our Monte Carlo data at high and low temperatures we compare the results for $H(\vec{r})$ with those for w . Note that

$$H(\vec{r}) = \langle [h(\vec{r}) - h(\vec{0})]^2 \rangle = 2w - 2\langle h(\vec{r})h(\vec{0}) \rangle, \quad (3.4)$$

and that as r approaches infinity at any temperature we expect

$$\langle h(\vec{r})h(\vec{0}) \rangle \rightarrow \langle h(\vec{r}) \rangle \langle h(\vec{0}) \rangle \rightarrow 0.$$

In Table I we list our Monte Carlo results for w and $H(r=16)$ for low and high temperatures, and the values for $\langle h(\vec{r})h(\vec{0}) \rangle$ at $r=16$ which follow from Eq. (3.4). For $T^* < 1.825$, $\langle h(16)h(0) \rangle$ is essentially zero. We conclude that the length associated with the decay of $\langle h(\vec{r})h(\vec{0}) \rangle$ is smaller than $r=16$, and that finite-size effects are negligible in this temperature range. At higher temperatures finite-size effects are significant, and can be estimated by calculating $\langle h(16)h(0) \rangle$ in the high-temperature approximation, as shown in Table I for $T^* > 2.0$.

In order to determine the temperature at which the roughening transition occurs, we look for the temperature at which the function $H(\vec{r})$ begins to diverge as r tends to infinity. Since in our finite system we have no true divergence, we look for a change in behavior. Qualitatively, such a change may be seen from Fig. 9 to have occurred between $T^* = 1.8$ and $T^* = 1.845$. We define r_{asym} as the smallest radius at which $H(\vec{r})$ is within 1% of its value at $r_0 = 12$. In Fig. 10 we plot r_{asym} as a function of temperature. The parameter r_{asym} measures the length associated with the decay of $\langle h(\vec{r})h(\vec{0}) \rangle$, and its abrupt increase as a function of temperature is a signature of the roughening transition. We tentatively identify the roughening temperature $T_1^* = 1.825 \pm 0.025$. Our estimate does not change significantly if we use $r_0 = 16$ as our reference point or if we replace 1% in our definition of r_{asym} by 0.5% or 2%.

The errors in r_{asym} are estimated by determining r_{asym} for blocks of 2000 passes and then averaging the values thus obtained and computing the standard deviation. Typical errors are shown in Fig. 10.

B. Orientational correlations

1. Tilt-tilt correlation function

The transition to an unoriented interface may be studied by computing the correlation of the tilt of the surface at one point with the tilt at a point a distance r away. Define¹⁰

$$g(\vec{r}) = \sum_j \langle [h(\vec{r}) - h(\vec{r} + \hat{\delta}_j) - h(\vec{0}) + h(\hat{\delta}_j)]^2 \rangle. \quad (3.5)$$

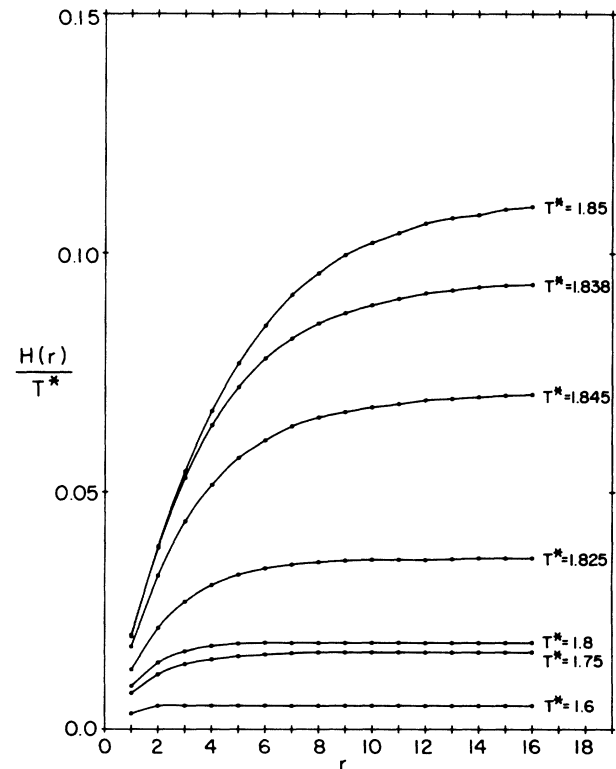


FIG. 9. Monte Carlo data for the height-height correlation function $H(r)$ as a function of separation r at various temperatures $T^* \leq 1.85$.

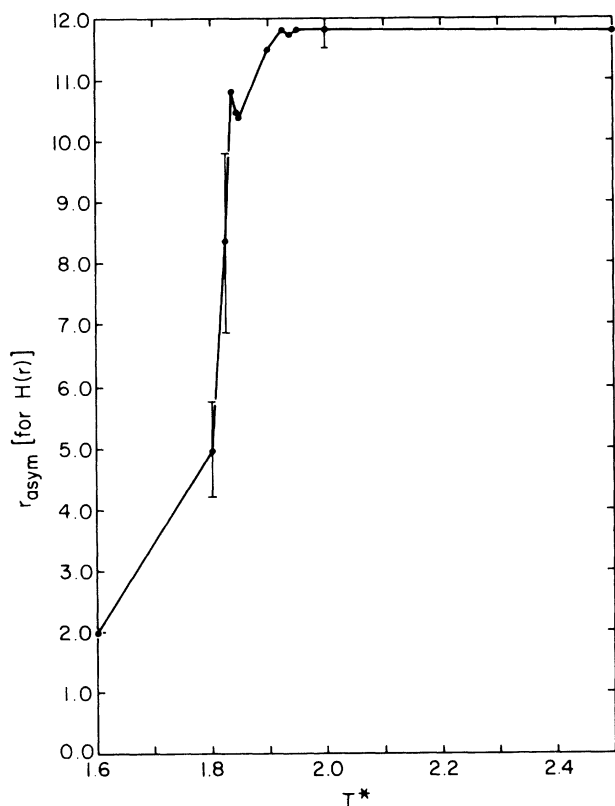


FIG. 10. Parameter r_{asym} , defined as the smallest radius at which the height-height correlation function $H(r)$ is within 1% of its value at $r_0=12$, as a function of temperature T^* .

Below the orientational transition $g(\vec{r})$ is expected to tend to a finite value at large r . In the thermodynamic limit $g(\vec{r})$ will diverge at large r above the orientational transition. In the high-temperature region $g(\vec{r})$ takes the form

$$g(\vec{r})/T^* = (6/N) \sum_{\vec{q}} G(\vec{q}) [1 - \exp(i\vec{q} \cdot \vec{r})]. \quad (3.6)$$

The integral approximation to (3.6) yields

$$g(r)/T^* = [3(3^{1/2})/2\pi] (\ln r + c). \quad (3.7)$$

In Fig. 11 our Monte Carlo results for $g(\vec{r})$ are shown, along with the high-temperature form (3.6) and its integral approximation (3.7). The constant c in (3.7) is chosen to give agreement with (3.6) at $r=1$. The results for $T^* > 2.0$ fit the finite-size high-temperature result (3.6) quite well. The integral approximation (3.7) is shown to be in good agreement with the finite-size exact sum (3.6) for $r < 8$. Discrepancies for larger values of r are due to finite-size effects. Despite the flattening due to these effects, $g(r)$ does not saturate until r is greater than 14. Saturation of $g(r)$ for smaller values of r is an indication of orientational order. From Fig. 11 we estimate that the orientational transition occurs between $T^*=1.9$ and $T^*=1.95$.

We now compute r_{asym} , the smallest radius at which $g(\vec{r})$ reaches values within 1% of $g(r=12)$. The results, shown in Fig. 12 as a function of temperature, confirm the

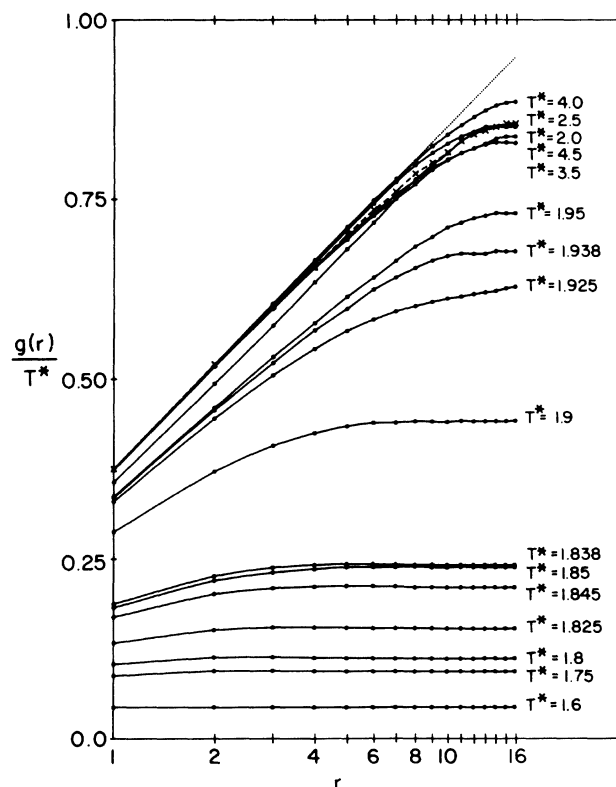


FIG. 11. Monte Carlo data for the tilt-tilt correlation function $g(r)$ as a function of the logarithm of the separation r at various temperatures T^* . The curve $\times \cdots \times$ represents the high-temperature approximation (3.6) for a finite system with periodic boundary conditions, and the curve \cdots represents the integral approximation (3.7) to the high-temperature result.

existence of an orientational transition at $T_2^* = 1.925 \pm 0.025$. Typical errors are estimated as for Fig. 10.

The quoted uncertainties in T_1^* and T_2^* reflect the temperature range within which the abrupt change in r_{asym} occurs. As shown in Fig. 13, the temperature shift between curves a and b is roughly constant and equal to 0.1 for $r_{\text{asym}} > 6$. Thus, although the determination of T_1^* and T_2^* is uncertain to within ± 0.025 , the temperature interval $T_2^* - T_1^*$ remains approximately equal to 0.1.

2. The correlation functions $c_k(r)$ and $c(r)$

The correlation function $c_k(\vec{r})$ is defined by¹⁰

$$c_k(r) = \left\langle \exp \left[2\pi i k \sum_j (-1)^j h(\vec{r}_j) \right] \right\rangle, \quad (3.8)$$

where the $\{\vec{r}_j\}$ are situated on a hexagon of size r [see Fig. 3(c)] and k is an arbitrary constant. The related correlation function

$$c(r) = - \frac{1}{(2\pi)^2} \left. \frac{\partial^2 c_k(r)}{\partial k^2} \right|_{k=0} = \left\langle \left[\sum_j (-1)^j h(\vec{r}_j) \right]^2 \right\rangle \quad (3.9)$$

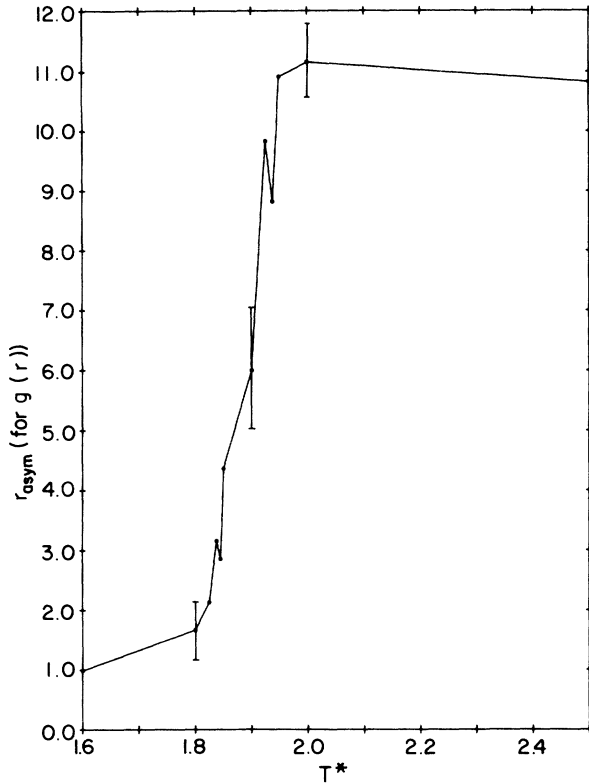


FIG. 12. Parameter r_{asym} , defined as the smallest radius at which the tilt-tilt correlation function $g(r)$ is within 1% of its value at $r_0=12$, as a function of temperature T^* .

is equal to τ in (2.8) for $r=1$. For arbitrary r , $c(r)$ measures orientational order within a hexagon of size r . This correlation function will remain finite at large r in the low-temperature, oriented phase, and will diverge for large r in the high-temperature, unoriented phase.

In the high-temperature region these correlation functions are given by

$$\begin{aligned} c(r) &= -\ln[c_k(r)]/(2\pi^2 k^2) \\ &= (T^*/N) \sum_{\vec{q}} G^2(\vec{q}) \left| \sum_j (-1)^j \exp(ir\vec{q} \cdot \hat{\delta}_j) \right|^2. \end{aligned} \quad (3.10)$$

The integral approximation to (3.10) yields

$$c(r) = T^* [3(3^{1/2})/8\pi] (\ln \frac{27}{16}) r^2. \quad (3.11)$$

Note that at high temperatures $c(r)$ diverges as the area of the enclosed hexagon and $c_k(r)$ decays exponentially with $(kr)^2$. Nelson¹⁰ has argued that the intermediate, quasicrystalline phase is characterized by algebraic decay of $c_k(r)$ and a logarithmic divergence of $c(r)$ as r approaches infinity.

Figure 14 shows our Monte Carlo results for $c_k(r)$ with $k=0.1$ and 0.125 . Small values of k correspond to slow decay of $c_k(r)$ with increasing r , and are preferable for numerical simulation. The r dependence of this correlation function is investigated for r up to 8, which corresponds to the largest hexagon that can be accommodated in a

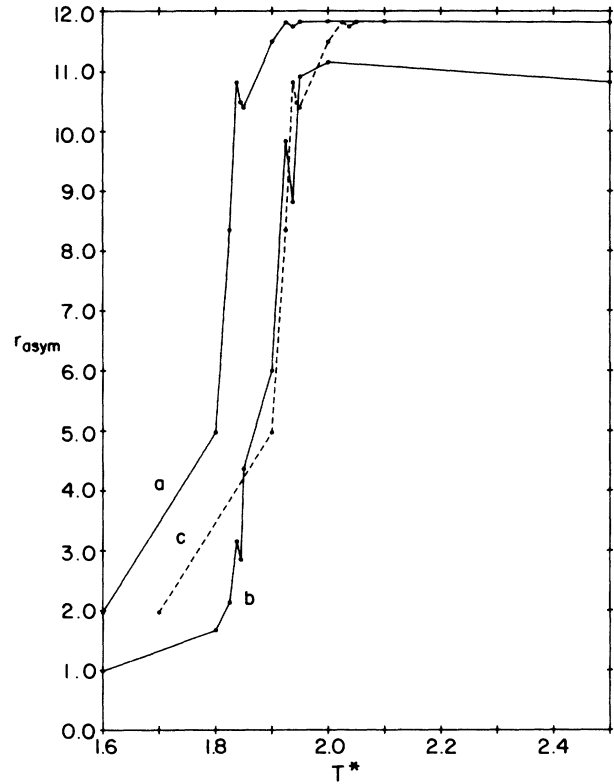


FIG. 13. Parameter r_{asym} as a function of temperature T^* . Curve *a* is the result computed from the height-height correlation function $H(r)$ (cf. Fig. 10). Curve *b* is the result computed from the tilt-tilt correlation function $g(r)$ (cf. Fig. 12). Curve *c* shows the result from $H(r)$ shifted in temperature by $\Delta T^*=0.1$.

32×32 lattice with periodic boundary conditions. For $T^* > 2.0$, the Monte Carlo results fit the high-temperature form (3.10) quite well and $c_k(r)$ is found to decay like the exponential of the area enclosed by the hexagon. As the temperature is lowered a weaker decay is observed, and saturation into a finite value for large r sets in for $T^* < 1.8$.

The behavior of the system at intermediate temperatures is investigated in Fig. 15 by plotting $\ln c_k(r)$ vs $\ln r$. The existence of a linear regime for $5 < r < 8$ signals algebraic decay of $c_k(r)$ in the temperature range $1.825 < T^* < 1.9$. Our Monte Carlo results for $c(r)$, shown in Fig. 16, also exhibit the asymptotic behavior $c(r) \sim \ln r$ for $1.825 < T^* < 1.925$. The saturation of $c(r)$ to a finite value for $T^* \leq 1.825$ is characteristic of orientational long-range order. For $T^* \geq 1.925$ orientational order is lost and $c(r)$ diverges faster than $\ln r$. These results support the existence of the intermediate phase for $1.825 < T^* < 1.925$, consistent with the estimated values of T_1^* and T_2^* obtained in Secs. III A and III B 1.

IV. DETERMINATION OF K AND K_A

The correlation functions defined in Sec. III may be written in the disclination language via a duality transformation.¹⁰ The expressions thus obtained can be interpreted in terms of a renormalized interaction between disclination test charges.¹⁰ In this section we use the predictions

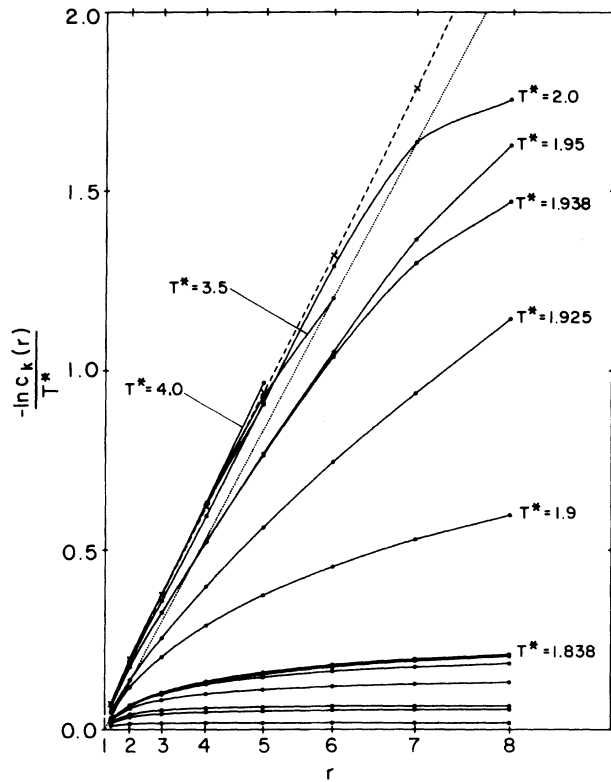


FIG. 14. Monte Carlo data for the logarithm of the orientational correlation function $c_k(r)$ for $k=0.125$ and $k=0.1$ as a function of the square of the separation r at various temperatures T^* . The curve $\times\text{---}\times$ represents the high-temperature approximation (3.10) for a finite system with periodic boundary conditions for $k=0.125$. The curve \cdots represents the integral approximation (3.11) to the high-temperature result for $k=0.125$.

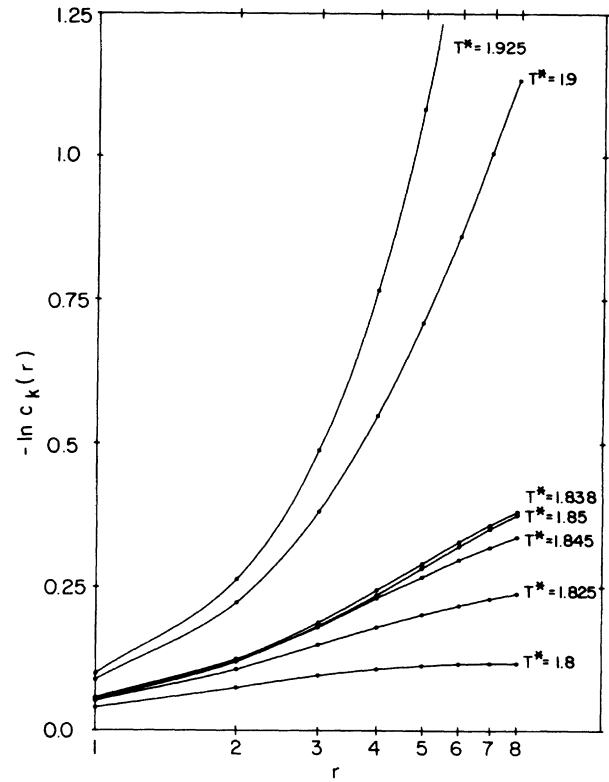


FIG. 15. Monte Carlo data for the logarithm of the orientational correlation function $c_k(r)$ for $k=0.125$ and $k=0.1$ as a function of the logarithm of the separation r at various temperatures $T^* \leq 1.925$.

of the KTHNY theory for two-dimensional melting¹³ to obtain finite-size forms for these correlation functions^{15,16} in the quasiooriented and unoriented phases. By fitting our Monte Carlo data to these forms we extract the temperature dependence of the elastic constant K and the Frank constant K_A .

In order to perform the duality transformation, it is convenient to introduce

$$g_k(\vec{r}) = \sum_j \langle \exp\{2\pi i k [h(\vec{r}) - h(\vec{r} + \hat{\delta}_j) - h(\vec{0}) + h(\hat{\delta}_j)]\} \rangle, \quad (4.1a)$$

$$c_k(r) = \left\langle \exp \left[2\pi i k \sum_j (-1)^j h(\vec{r}_j) \right] \right\rangle, \quad (4.1b)$$

$$H_k(\vec{r}) = \langle \exp\{2\pi i k [h(\vec{r}) - h(\vec{0})]\} \rangle. \quad (4.1c)$$

The correlation functions defined in Sec. III are thus given by

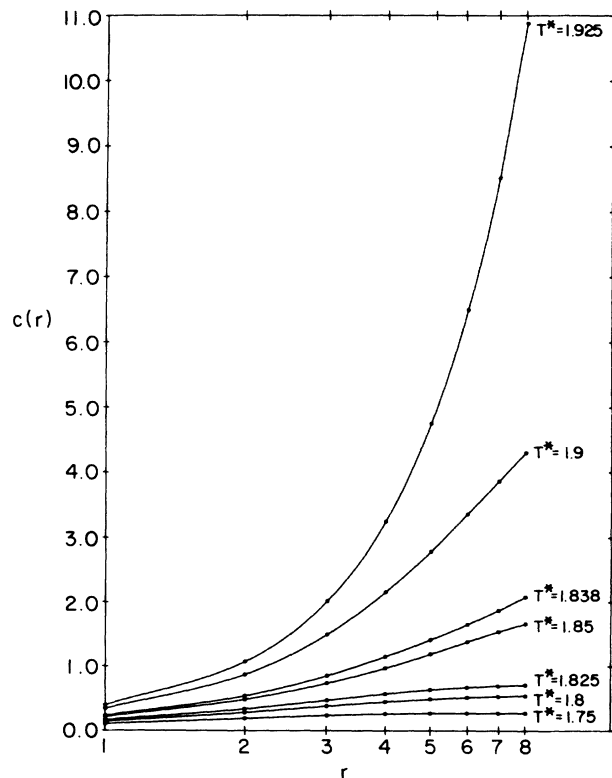


FIG. 16. Monte Carlo data for the orientational correlation function $c(r)$ as a function of the logarithm of the separation r at various temperatures $T^* \leq 1.925$.

$$g(\vec{r}) = -\frac{1}{(2\pi)^2} \frac{\partial^2 g_k(\vec{r})}{\partial k^2} \Big|_{k=0}, \quad (4.2a)$$

$$H(\vec{r}) = -\frac{1}{(2\pi)^2} \frac{\partial^2 H_k(\vec{r})}{\partial k^2} \Big|_{k=0}. \quad (4.2c)$$

$$c(r) = -\frac{1}{(2\pi)^2} \frac{\partial^2 c_k(r)}{\partial k^2} \Big|_{k=0}, \quad (4.2b)$$

The orientational correlation functions (4.1a) and (4.1b) transform via duality into¹⁰

$$g_k(\vec{r}) = \sum_j \exp\{- (2\pi)^2 T^* k^2 [-2V(\vec{r}) - 2V(\hat{\delta}_j) + V(\vec{r} + \hat{\delta}_j) + V(\vec{r} - \hat{\delta}_j)]\} \\ \times \left\langle \exp \left[(2\pi)^2 T^* k \sum_{\vec{r}'} s(\vec{r}') [-V(\vec{r}' - \vec{r}) + V(\vec{r}' - \vec{r} - \hat{\delta}_j) + V(\vec{r}') - V(\vec{r}' - \hat{\delta}_j)] \right] \right\rangle_d \quad (4.3a)$$

and

$$c_k(r) = \exp \left[- (2\pi)^2 (T^* k^2 / 2) \sum_{j \neq j'} (-1)^{(j+j')} V(\vec{r}_j - \vec{r}_{j'}) \right] \left\langle \exp \left[(2\pi)^2 T^* k \sum_{\vec{r}'} s(\vec{r}') \sum_j (-1)^j V(\vec{r}_j - \vec{r}') \right] \right\rangle_d, \quad (4.3b)$$

where $\langle \dots \rangle_d$ implies an average over a disclination ensemble subject to the neutrality constraints (1.7). The interaction between disclinations in this ensemble is given by $V(\vec{r})$ defined by (1.6). The forms (4.3) allow us to interpret these correlation functions in terms of the free energy of configurations of disclination test charges situated as in Figs. 3(b) and 3(c).¹⁰ In both cases the prefactor measures the bare interaction between the test charges of strength k , and the second factor is due to interactions between these test charges and thermally excited disclinations. At low temperatures \tilde{T} in the disclination ensemble [high T^* , see (1.9)] there are no thermally excited disclinations, and thus the prefactors in (4.3) reproduce the high- T^* results of Sec. III.

The height-height correlation function (4.1c) transforms via duality into

$$H_k(\vec{r}) = \exp\{- (2\pi)^2 T^* k^2 [U(\vec{r}) - V(\vec{r})]\} \left\langle \exp \left[(2\pi)^2 T^* k \sum_{\vec{r}'} s(\vec{r}') [V(\vec{r}' - \vec{r}) - V(\vec{r}') - U(\vec{r}' - \vec{r}) + U(\vec{r}')] \right] \right\rangle_d, \quad (4.4)$$

where $\langle \dots \rangle_d$ implies an average over a disclination ensemble subject only to the charge neutrality condition (1.7a). The interaction between disclinations in this ensemble is given by $V(\vec{r}) - U(\vec{r})$, where

$$U(\vec{r}) = (1/2N) \sum_{\vec{q}} G^2(\vec{q}) (\vec{q} \cdot \vec{r})^2. \quad (4.5)$$

The form (4.4) allows us to interpret this correlation function in terms of the free energy of a pair of disclinations of strength k separated by a distance r [see Fig. 3(a)]. The prefactor measures the bare interaction between the test charges, and the second factor is due to interactions between these test charges and thermally excited disclinations. The prefactor can be shown to reproduce the high-temperature result (3.2) by substituting (1.6) and (4.5) into (4.4). The function $U(r)$ diverges like $\ln N$ in the thermodynamic limit. Thus the function $H(\vec{r})$ diverges for all r in the thermodynamic limit at high T^* . As T^* is lowered below T_2^* , the screening due to thermally excited disclinations results in a finite $H(\vec{r})$ for finite r . These divergences cannot be observed in a Monte Carlo simulation of a finite system.

The correlation functions (4.1) measure the response of the disclination system to the externally imposed configurations of test disclinations shown in Fig. 3. The corresponding correlation functions (4.2) measure this response

in the limit in which the strength k of the test disclinations approaches zero.

The KTHNY theory for the disclination system in the solid and hexatic phases yields specific predictions for the behavior of the correlation functions (4.1) and (4.2) in the rough, unoriented and rough, quasioriented phases.¹⁰ For a finite system with periodic boundary conditions the KTHNY predictions in the rough unoriented phase are

$$H(\vec{r}) = [K_R / 2(3^{1/2})\pi^2] (1/N) \\ \times \sum_{\vec{q}} G^2(\vec{q}) |1 - \exp(i\vec{q} \cdot \vec{r})|^2, \quad (4.6a)$$

$$g(\vec{r}) = [K_R / 2(3^{1/2})\pi^2] (1/N) \\ \times \sum_{\vec{q}} G^2(\vec{q}) \sum_j |1 - \exp(i\vec{q} \cdot \hat{\delta}_j)|^2 \\ \times |1 - \exp(i\vec{q} \cdot \vec{r})|^2, \quad (4.6b)$$

$$c(r) = [K_R / 2(3^{1/2})\pi^2] (1/N) \\ \times \sum_{\vec{q}} G^2(\vec{q}) \left| \sum_j (-1)^j \exp(ir\vec{q} \cdot \hat{\delta}_j) \right|^2, \quad (4.6c)$$

where the wave vectors \vec{q} are appropriate to the finite system and K_R is the renormalized elastic constant.

The high-temperature results of Sec. III are recovered for

$$K_R \rightarrow K = 2(\pi)^2(3^{1/2})T^* .$$

As T^* approaches T_2^* from above, screening effects due to thermally excited dislocations do not change the \vec{r} dependence of the correlation functions (4.6). In this regime, the screening effects can be completely accounted for by the temperature dependence of the renormalized elastic constant K_R .² As T^* approaches T_2^* from above, K_R approaches the universal value 16π .^{2,3,10} We extract K_R by fitting our Monte Carlo data for the correlation functions to the finite-size forms (4.6). The results for K_R as a function of temperature are shown in Fig. 17. For $T^* > 2.0$ the data is in good agreement with the high-temperature prediction $K_R = 2(\pi)^2(3^{1/2})T^*$. Below $T^* = 2.0$, K_R drops abruptly, and goes through 16π at $T_2^* = 1.925 \pm 0.015$, in agreement with our previous estimate of T_2^* in Sec. III B 1.

The presence of free dislocations in the hexatic phase produces a screened, logarithmic interaction between disclinations.² In this regime the disclination system is described by an effective Hamiltonian

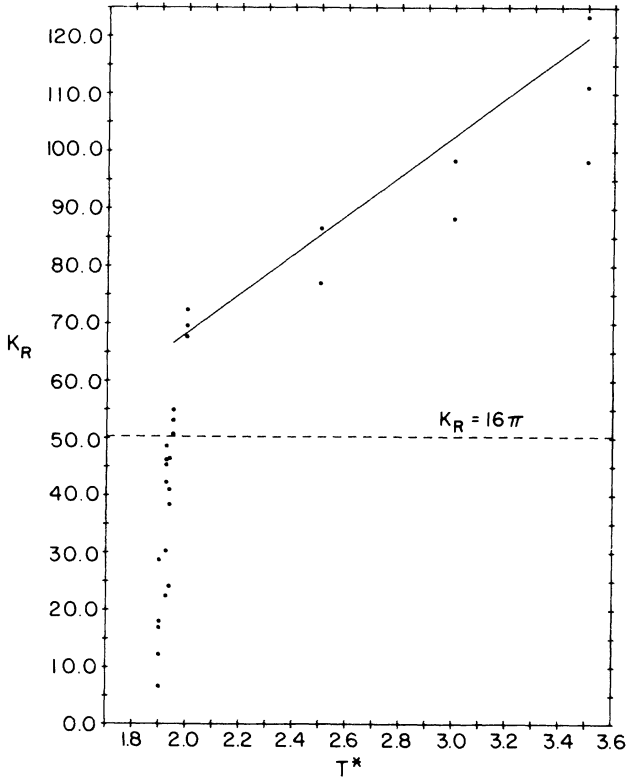


FIG. 17. Renormalized elastic constant K_R as a function of temperature T^* as obtained from fits of the correlation functions $H(r)$, $g(r)$, $c_k(r)$, and $c(r)$ to the forms (4.6). Different points at a given temperature represent determinations from different correlation functions and/or different Monte Carlo runs. The solid line represents the high-temperature result $K_R = 2(\pi)^2(3^{1/2})T^*$.

$$H = \pi K_A / 36 \sum_{\vec{r} \neq \vec{r}'} s(\vec{r}) s(\vec{r}') W(\vec{r} - \vec{r}') , \quad (4.7)$$

where K_A is the Frank elastic constant and the interaction $W(\vec{r})$ is given in terms of the triangular lattice Green's function (1.4) by

$$W(\vec{r}) = (4\pi/3^{1/2})(1/N) \sum_{\vec{q}} G(\vec{q}) [\exp(i\vec{q} \cdot \vec{r}) - 1] . \quad (4.8)$$

For a finite system with periodic boundary conditions the KTHNY predictions in the rough, quasioiented phase are

$$\begin{aligned} H(\vec{r}) &= 2A(T) + [K_A/18(3^{1/2})](1/N) \\ &\quad \times \sum_{\vec{q}} G(\vec{q}) |1 - \exp(i\vec{q} \cdot \vec{r})|^2 , \quad (4.9a) \\ g(\vec{r}) &= 24A(T) + [K_A/18(3^{1/2})](1/N) \\ &\quad \times \sum_{\vec{q}} G(\vec{q}) \sum_j |1 - \exp(i\vec{q} \cdot \hat{\delta}_j)|^2 \\ &\quad \times |1 - \exp(i\vec{q} \cdot \vec{r})|^2 , \quad (4.9b) \end{aligned}$$

$$c(r) = 6A(T) + [K_A/18(3^{1/2})](1/N)$$

$$\times \sum_{\vec{q}} G(\vec{q}) \left| \sum_j (-1)^j \exp(ir\vec{q} \cdot \hat{\delta}_j) \right|^2 , \quad (4.9c)$$

where $A(T)$ is related to the renormalized core energy for disclinations in this phase. The KTHNY theory predicts that K_A diverges as T^* approaches T_2^* from below, and that K_A approaches the universal value $72/\pi$ as T^* tends to T_1^* from above.^{2,10} Since

$$\sum_j |1 - \exp(i\vec{q} \cdot \hat{\delta}_j)|^2 = 3G^{-1}(\vec{q}) ,$$

$g(\vec{r})$ rapidly approaches a finite asymptotic value with increasing r , reflecting the finite energy required to unbind a dislocation pair. The correlation functions $H(\vec{r})$ and $c(r)$ increase logarithmically with r in the thermodynamic limit, reflecting the quasi-long-range orientational order characteristic of the intermediate phase.

We extract K_A by fitting our Monte Carlo data for the correlation functions $H(\vec{r})$ and $c(r)$ to the corresponding finite-size forms (4.9). The function $g(\vec{r})$ cannot be used for this purpose because it exhibits a weak r dependence and its asymptotic value depends on both K_A and $A(T)$. For $H(\vec{r})$ and $c(r)$ we obtain a good fit to the forms (4.9a) and (4.9c) for $T^* \leq 1.9$, while at higher temperatures the r dependence of the correlation functions changes and corresponds to the forms (4.6). This change is illustrated in Fig. 18. The results for K_A as a function of temperature are shown in Fig. 19. Below T_2^* , K_A decreases rapidly

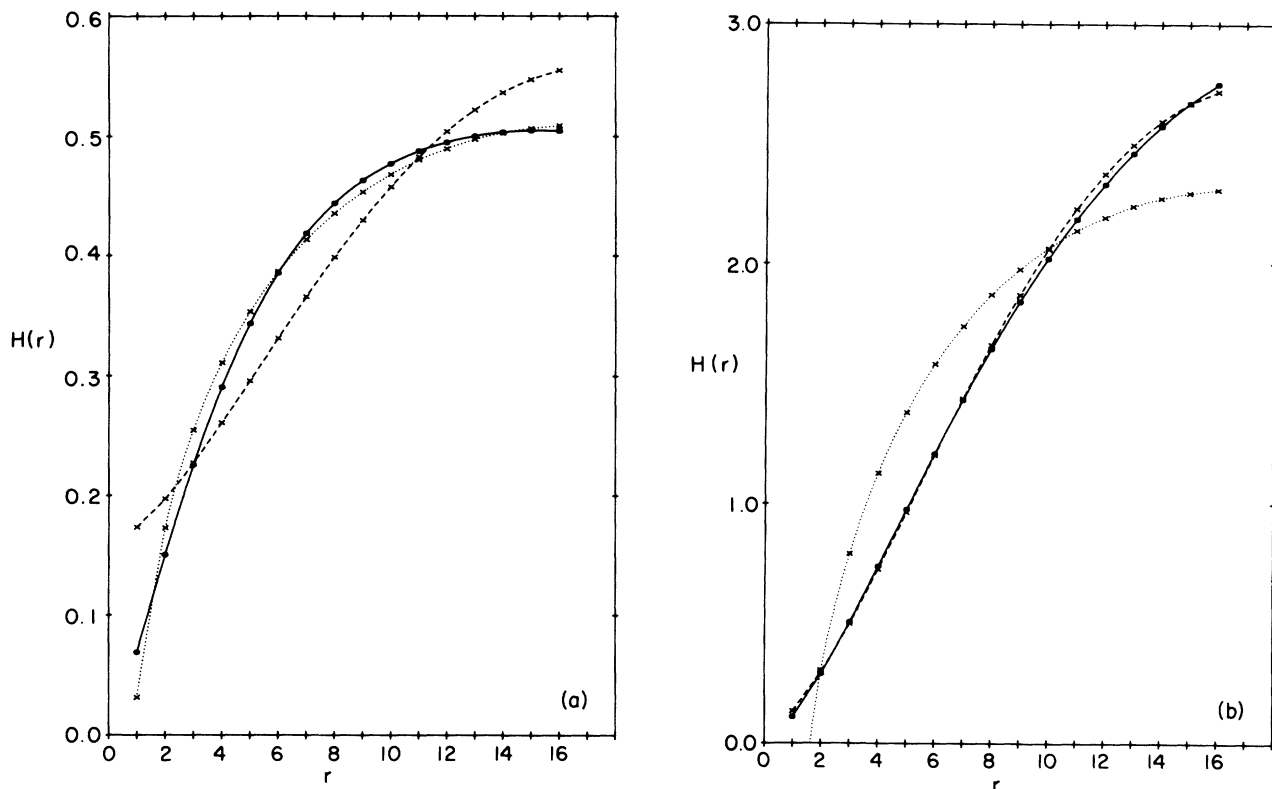


FIG. 18. Monte Carlo data for the height-height correlation function $H(r)$ at (a) $T^* = 1.9$ and (b) $T^* = 1.925$. Best fits to the forms (4.6a) and (4.9a) are denoted by $\times\text{---}\times$ and $\times\cdots\times$, respectively. Note the crossover from behavior at $T^* = 1.925$, characteristic of the rough, unoriented phase, to that at $T^* = 1.9$, characteristic of the rough, quasiooriented phase.

with decreasing T^* , and goes through $72/\pi$ at $T_1^* = 1.84 \pm 0.01$, in agreement with our previous estimate of T_1^* in Sec. III A.

V. SUMMARY AND CONCLUSIONS

We have investigated the thermodynamic properties of the Laplacian roughening model over the full temperature range. Analytic results obtained in the low- and high-temperature limits are in excellent agreement with the corresponding simulation data. Our Monte Carlo results for the correlation functions indicate the existence of a rough, quasiooriented phase at intermediate temperatures. Duality arguments which establish the correspondence between this roughening model and a disclination system identify the intermediate phase as the hexatic phase of the disclination system.¹⁰

The transition from the smooth, oriented phase into the rough, quasiooriented phase occurs at $T_1^* = 1.84 \pm 0.01$. The orientational transition into a rough, unoriented phase occurs at $T_2^* = 1.925 \pm 0.015$. Our simulations present strong evidence for the existence of the intermediate phase within a temperature range $\Delta T^* = T_2^* - T_1^* \cong 0.09$. Monte Carlo simulations of the Laplacian roughening model on a square lattice have also indicated the existence of an intermediate phase.¹⁸

The internal energy, interface width, and local orientation are found to be smooth functions of temperature.

These thermodynamic quantities exhibit no discontinuity or hysteresis, so there is no indication of a first-order phase transition. The rather sharp specific heat peak at $T^* \cong 1.85$ could be due to a single second-order phase transition, a possibility that cannot be ruled out on the basis of thermodynamic functions only. However, this peak is also consistent with the picture of two KT transitions separated by a narrow temperature range. Such a description predicts unobservable essential singularities in thermodynamic quantities at T_1^* and T_2^* .^{1,2,10} The specific heat peak is then caused by the gradual dissociation of bound pairs of dislocations and disclinations with decreasing T^* (increasing \tilde{T}), and its location does not identify a transition temperature.¹⁹

The correlation functions calculated in this Monte Carlo simulation provide the essential information needed to characterize the phases and detect the phase transitions. Our results confirm the predictions of the KTHNY theory for the disclination system. Their theory is based on an expansion in the fugacity $y = \exp(-E_c/k_B \tilde{T})$ and is expected to break down at small core energy.¹⁵ The Laplacian roughening model corresponds via duality to a disclination system of core energy $E_c/k_B \tilde{T} = BK/16\pi$.¹⁰ The parameter B , which controls the core energy, is determined by the interaction $V(\vec{r})$ between disclinations, Eq. (1.8). We compute B from the upper transition temperature T_2^* using the HNY recursion relations^{2,3} to obtain B approximately equal to 2.1. A fit of $V(\vec{r})$ in (1.6) to the

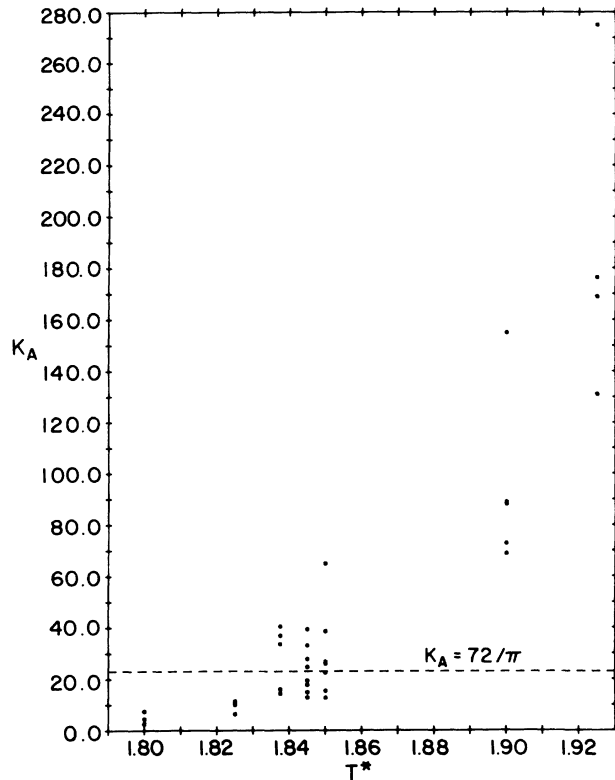


FIG. 19. Frank elastic constant K_A as a function of temperature T^* as obtained from fits of the correlation functions $H(r)$, $c_k(r)$, and $c(r)$ to the forms (4.9). Different points at a given temperature represent determinations from different correlation functions and/or different Monte Carlo runs.

form (1.8) does not yield an independent estimate of B , since the resulting value is too sensitive to details of the fitting procedure. A consistency check follows from the observation that the form (1.8) with $B = 2.1$ provides a good fit to (1.6) (and yields $A = 1.9$).

The core energy for thermal excitation of dislocations, determined by the parameter B , is of interest because there is evidence that it may control the crossover from a KT to a first-order transition in these systems.^{15,20} Saito's results from direct simulation of the dislocation system imply that the transition is continuous for $B > 1.63$ and first or-

der for $B < 1.13$. The parameter B is generally not known for atomic models. The value $B = 2.44$ obtained by Fisher, Halperin, and Morf²¹ for the two-dimensional electron system suggests a continuous phase transition for that system. Since $B \approx 2.1$ for the Laplacian roughening model, our observation of two continuous transitions is consistent with Saito's results.

The transitions of the Laplacian roughening model have been located, and their relation to the transitions of the dual disclination system¹⁰ has been established. The Monte Carlo results for the correlation functions are fit well by the predictions of the KTHNY theory for a finite system with periodic boundary conditions, and yield the temperature dependence of the renormalized elastic coupling K_R and the Frank constant K_A . The rough, unoriented phase (corresponding to the solid) is characterized by a finite value of K_R and an infinite value of K_A . K_R decreases with decreasing T^* (increasing \tilde{T}) and takes the universal value 16π at the transition temperature $T_2^* = 1.925 \pm 0.015$ (corresponding to the dislocation unbinding transition). The rough, quasioriented phase (corresponding to the hexatic phase) is characterized by a finite K_A and a vanishing K_R . K_A decreases with decreasing T^* (increasing \tilde{T}) and takes the value $72/\pi$ at the transition temperature $T_1^* = 1.84 \pm 0.01$ (corresponding to the disclination unbinding transition). Both K_A and K_R vanish in the smooth, oriented phase (corresponding to the isotropic fluid).

Our simulations have established the existence of a rough, quasioriented phase at intermediate temperatures. This phase only exists within a narrow temperature range, in agreement with the recent experimental observation of the hexatic phase.⁹ An interesting open problem is that of stabilizing the intermediate phase over a wider temperature range by allowing for generalizations of the Laplacian roughening model considered here.

ACKNOWLEDGMENTS

We have benefited from conversations with D. R. Nelson and D. A. Bruce. This research was supported in part by Grant No. DMR-79-24008-A02 from the National Science Foundation, administered through the Materials Science Center at Cornell University.

¹J. M. Kosterlitz and D. J. Thouless, *J. Phys. C* **6**, 1181 (1973).
²B. I. Halperin and D. R. Nelson, *Phys. Rev. Lett.* **41**, 121 (1978); **41**, 519 (E) (1978).
³D. R. Nelson and B. I. Halperin, *Phys. Rev. B* **19**, 2457 (1979).
⁴A. P. Young, *Phys. Rev. B* **19**, 1855 (1979).
⁵W. F. Brinkman, D. S. Fisher, and D. E. Moncton, *Science* **217**, 693 (1982).
⁶See, for instance, work reported in *Ordering in Two Dimensions*, edited by S. K. Sinha (North-Holland, New York, 1980), and *Melting, Localization, and Chaos*, edited by R. K. Kalia and P. Vashishta (North-Holland, New York, 1982).
⁷R. Pindak, D. J. Bishop, and W. O. Sprenger, *Phys. Rev. Lett.*

44, 1461 (1980); R. Pindak, D. E. Moncton, S. C. Davey, and J. W. Goodby, *ibid.* **46**, 1135 (1981).
⁸P. A. Heiney, R. J. Birgeneau, G. S. Brown, P. M. Horn, D. E. Moncton, and P. W. Stephens, *Phys. Rev. Lett.* **48**, 104 (1982).
⁹T. F. Rosenbaum, S. E. Nagler, P. M. Horn, and R. Clarke, *Phys. Rev. Lett.* **50**, 1791 (1983).
¹⁰D. R. Nelson, *Phys. Rev. B* **26**, 269 (1982).
¹¹S. T. Chui and J. D. Weeks, *Phys. Rev. B* **14**, 4978 (1976); H. J. F. Knops, *Phys. Rev. Lett.* **39**, 766 (1977); J. V. José, L. P. Kadanoff, S. Kirkpatrick, and D. R. Nelson, *Phys. Rev. B* **16**, 1217 (1977).

- ¹²R. H. Swendsen, Phys. Rev. B 18, 492 (1978); W. J. Shugard, J. D. Weeks, and G. H. Gilmer, Phys. Rev. Lett. 41, 1399 (1978); W. J. Shugard, J. D. Weeks, and G. H. Gilmer, Phys. Rev. B 21, 5309 (1980). For a review, see J. D. Weeks, in *Ordering in Strongly Fluctuating Condensed Matter Systems*, edited by T. Riste (Plenum, New York, 1980), p. 293.
- ¹³For reviews, see B. I. Halperin, in Proceedings of the Kyoto Summer Institute 1979—Physics of Low Dimensional Systems, edited by Y. Nagaoka and S. Hikami (Publication Office, Progress of Theoretical Physics, Kyoto, 1979), p. 53; D. R. Nelson, in *Proceedings of the 1980 Summer School on Fundamental Problems in Statistical Mechanics, Enschede*, edited by E. G. D. Cohen (North-Holland, Amsterdam, 1980).
- ¹⁴S. T. Chui, Phys. Rev. Lett. 48, 933 (1982).
- ¹⁵Y. Saito, Phys. Rev. Lett. 48, 1114 (1982); Phys. Rev. B 26, 6239 (1982).
- ¹⁶Y. Saito and H. Müller-Krumbhaar, Phys. Rev. B 23, 308 (1981); W. J. Shugard, J. D. Weeks, and G. H. Gilmer, *ibid.* 25, 2022 (1982).
- ¹⁷R. H. Swendsen, Phys. Rev. B 15, 5421 (1977).
- ¹⁸D. A. Bruce (private communication).
- ¹⁹S. A. Solla and E. K. Riedel, Phys. Rev. B 23, 6008 (1981).
- ²⁰R. H. Swendsen, Phys. Rev. Lett. 49, 1302 (1982).
- ²¹D. S. Fisher, B. I. Halperin, and R. Morf, Phys. Rev. B 20, 4692 (1979).